Computer modeling of fibrin polymerization kinetics correlated with electron microscope and turbidity observations: clot structure and assembly are kinetically controlled

John W. Weisel and Chandrasekaran Nagaswami
Department of Anatomy, University of Pennsylvania School of Medicine, Philadelphia, Pennsylvania 19104-6058 USA

ABSTRACT Although much is known about fibrin polymerization, because it is complex, the effects of various modifications are not intuitively obvious and many experimental observations remain unexplained. A kinetic model presented here that is based on information about mechanisms of assembly accounts for most experimental observations and allows hypotheses about the effects of various factors to be tested. Differential equations describing the kinetics of polymerization were written and then solved numerically. The results have been related to turbidity profiles and electron microscope observations. The concentrations of intermediates in fibrin polymerization, and fiber diameters, fiber and protofibril lengths have been calculated from these models. The simplest model considered has three steps: fibrinopeptide A cleavage, protofibril formation, and lateral aggregation of protofibrils to form fibers. The average number of protofibrils per fiber, which is directly related to turbidity, can be calculated and plotted as a function of time. The lag period observed in turbidity profiles cannot be accurately simulated by such a model, but can be simulated by modifying the model such that oligomers must reach a minimum length before they aggregate. Many observations, reported here and elsewhere, can be accounted for by this model; the basic model may be modified to account for other experimental observations. Modeling predicts effects of changes in the rate of fibrinopeptide cleavage consistent with electron microscope and turbidity observations. Changes only in the rate constants for initiation of fiber growth or for addition of protofibrils to fibers are sufficient to account for a wide variety of other observations, e.g., the effects of ionic strength or fibrinopeptide B removal or thrombospondin. The effects of lateral aggregation of fibers has also been modeled: such behavior has been observed in turbidity curves and electron micrographs of clots formed in the presence of platelet factor 4. Thus, many aspects of clot structure and factors that influence structure are directly related to the rates of these steps of polymerization, even though these effects are often not obvious. Thus, to a large extent, clot structure is kinetically determined.

INTRODUCTION

Fibrinogen is the key structural protein in blood clotting. It is a fibrous protein with a molecular mass of 340 kD made up of three pairs of polypeptide chains held together by disulfide bonds. Fibrinogen is converted to fibrin by enzymatic cleavage of the fibrinopeptides by thrombin; the pair of A fibrinopeptides is removed first, usually followed by the pair of B fibrinopeptides as the clot is formed. Fibrin monomers aggregate in a half staggered manner via complementary binding sites to form small oligomers which grow into longer structures, called two-stranded protofibrils. Protofibrils then aggregate laterally to produce fibers, which are paracrystalline structures with a distinctive band pattern. Fibers aggregate with each other to a variable extent depending on the ionic conditions to form fiber bundles, which branch, yielding a three-dimensional network or gel.

Many of these structures have been observed by electron microscopy, revealing details of the structures and the assembly process. Clot formation is commonly monitored by the measurement of turbidity as a function of time. The coordinated use of both light scattering or turbidity, which measures average parameters well, with electron microscopy, which is better for direct visualization of the detailed structures, is powerful. The kinetics of early events in clot formation, such as the cleavage of the A and B fibrinopeptides and the formation of small oligomers, have been investigated (e.g., Janmey, et al., 1983; Lewis, et al., 1985; Wilf and Minton, 1986; Sato and Nakajima, 1984; Wolfe and Waugh, 1981). The shape of the typical turbidity curves observed in clot formation has been analyzed (Hantgan and Hermans, 1979). There is a lag period which corresponds to the time required for the formation and growth of protofibrils from fibrin monomer after the removal of fibrinopeptides. The rapid rise in turbidity results from lateral aggregation of protofibrils that have reached a certain minimum length. The final value of turbidity when it levels off is related directly to the average size of the fibers or fiber bundles. It has been demonstrated that clot turbidity is directly proportional to the average cross-sectional area of the fibers comprising it (Carr and Hermans, 1978).

Much experimental work has been performed on the effects of various modifications of clotting conditions on the shape of the turbidity curves; a few examples will be noted here. Ferry and Morrison (1947) first investigated the effects of modification of ionic conditions on the turbidity curves, and many other studies followed. The influence of many components that are normally present in blood has also been investigated. Some examples include: calcium (Hardy, et al., 1983; Carr, et al., 1986), dextran (Dhall, et al., 1976; Carr and Gabriel, 1980), immunoglobulin (Gabriel, et al., 1983), albumin (Wilf, et al., 1985; Galanakis, et al., 1987), hydroxyethyl starch (Carr, 1986), platelet factor 4 (Carr, et al., 1987), thrombospondin (Bale and Mosher, 1986), collagen

Address correspondence to Dr. Weisel.

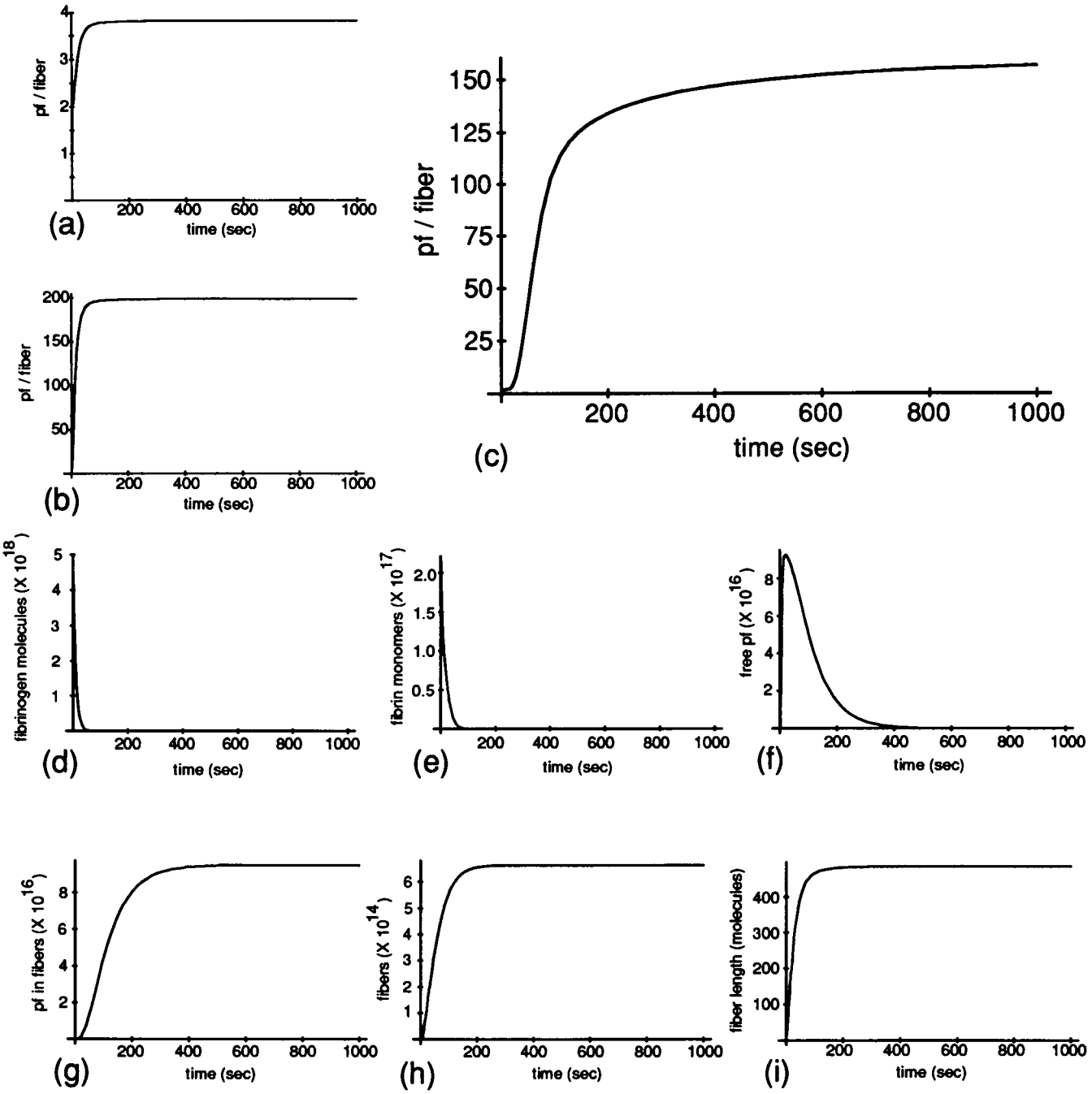

FIGURE 1 Modeling of the kinetics of fibrin polymerization. (*a*) Three-step mechanism: fibrinopeptide A cleavage; initiation and growth of protofibrils; initiation and growth of fibers. Here, the rate of growth of fibers is the same as the rate of initiation ($k_{fg} = k_{fi}$): $k_A = 1\ s^{-1}$ (N.B. measured values are larger, but there is no change in the curves for any value larger than this); $k_{pi} = k_{pg} = 4 \times 10^{-18}$ L/molecule s (N.B., this is the rate constant measured by Hantgan and Hermans, 1979); $k_{fi} = k_{fg} = 10^{-18}$ L/molecule s. (Note that the units of the rate constants for the calculations must be in number units rather than moles, but they can be converted to those normally used in biochemical kinetics simply by multiplying by Avogadro's number.) The average number of protofibrils per fiber (pf/fiber) rises rapidly and then levels off to a low number. (*b*) The results of the same three-step mechanism are shown here, but now fiber growth is more rapid than initiation ($k_{fg} > k_{fi}$): $k_{fi} = 10^{-21}$ L/molecule s; $k_{fg} = 2 \times 10^{-17}$ L/molecule s (all other rate constants are the same). The average number of pf/fiber rises rapidly and levels off at a much higher value. (*c*) The curve resulting from a model in which small oligomers cannot aggregate, but protofibrils must reach a certain length before they can aggregate to form fibers; in this case protofibrils can start aggregating when they contain at least 11 monomers. The length of the lag period is dependent on the minimum size oligomer that can aggregate. The rate constants, which also apply to all subsequent figures unless specified otherwise, are: $k_A = 1\ s^{-1}$ (N.B., again, there is no change in the curves for any value larger than this); $k_{pi} = 4 \times 10^{-18}$ L/molecule s (in this case, all oligomers were assumed to associate at this same rate with other oligomers of the same size and with protofibrils); $k_{pg} = 10^{-16}$ L/molecules s; $k_{fi} = 10^{-21}$ L/molecule s; $k_{fg} = 2 \times 10^{-17}$ L/molecule s. (*d*) The concentration of fibrinogen molecules as a function of time. The initial fibrinogen concentration is 5×10^{18} mol/L (or

(Jones and Gabriel, 1988), and poly (L-amino acids) (Carr, et al., 1989). These results are significant for several reasons. Studies of modifications to the physical or chemical properties of clots or the assembly process may help to elucidate the mechanisms of assembly. Also, it has been shown that clots produced in plasma are different than those formed with purified fibrinogen and thrombin (Shah, et al., 1987; Carr, 1988; Nair and Dhall, 1991), but exactly which plasma components are responsible for these differences is not entirely known. Finally, it is known that clots formed in vivo can be different in certain conditions; some of the proteins just mentioned may be present in different amounts under certain circumstances and may thus be responsible for modulating clot structure.

Furthermore, modifications to fibrinogen itself also affect the assembly process. Studies of the assembly properties of these modified preparations may yield insight into the function of different portions of the molecule. Examples include desialated or deglycosylated fibrinogen (Martinez, et al., 1977; Dang, et al., 1989; Langer, et al., 1988) and many proteolytic derivatives. Some of the results from such variations as those mentioned above are easily interpreted, but others are much more complicated and difficult to understand. In this paper, we develop a framework to help interpret the results of such experiments and provide examples and experimental evidence in the form of electron microscopy and turbidity curves for the effects of various modifications to the fibrin clotting system.

MATERIALS AND METHODS

Highly purified, plasminogen-free human fibrinogen (97–98% clottable) was obtained from Imco Co. (Stockholm, Sweden). Unless otherwise stated, all experiments were carried out in 0.15 M NaCl, 0.05 M Tris-HCl, pH 7.4, 1 mM $CaCl_2$ at 22°C, using fibrinogen concentrations 0.5–1.5 mg/mL. Clotting was initiated by the addition of thrombin, often to a final concentration of about 1 NIH unit/mL, but in some experiments the thrombin concentration was varied, as described in the text or figure legends. Turbidity was measured on a Lambda 4B spectrophotometer (Perkin-Elmer Corp., Norwalk, CT) at 350 nm and 22°C. After equilibration of fibrinogen in the appropriate buffer, and sometimes with another protein (as noted in the text), the absorbance at 350 nm was adjusted to 0 and freshly prepared thrombin was added at time 0. The optical density was sampled every 0.1 min and measured until there was little or no further change, usually within 120 min. Each experiment was repeated several times and data points were averaged.

Platelet factor 4 (Holt and Niewiarowski, 1989) was a generous gift of Drs. J. Holt and S. Niewiarowski (Thrombosis Research Center, Temple University School of Medicine, Philadelphia, PA). Thrombospondin (Tuszynski, et al., 1987) was a generous gift of Dr. G. Tuszynski (Department of Medicine, Medical College of Pennsylvania, Philadelphia, PA).

Fibrin monomer was prepared by the treatment of fibrinogen with thrombin and subsequent dissolution of the resulting clot at 4°C in acetic acid solution at pH 3.5 (Medved', et al., 1990). Protofibrils were formed by 10-fold dilution of concentrated (0.4 mg/mL) acidic monomer in 0.02 M phosphate buffer, pH 7.4, 0.2 M NaCl, 0.1 mM $CaCl_2$ at 37°C. With these conditions, polymerization was relatively slow, which allowed the preparation of samples for electron microscopy at various times during the fibrin clot formation process (Medved', et al., 1990). Because large numbers of protofibrils are present during the lag period of the turbidity curves, samples were taken for microscopy during this time.

Samples were prepared for transmission electron microscopy by the methods of either negative contrast or rotary shadowing. Negatively contrasted specimens of individual molecules, protofibrils or fibers were prepared by placing a drop on a glow-discharged carbon film and adding 1% uranyl acetate (Weisel, 1986*a*; Medved', et al., 1990). Preformed clots were applied to 300 mesh, glow-discharged carbon-coated Formvar grids and then negatively contrasted with uranyl acetate. Rotary-shadowed samples were prepared by spraying a dilute solution of molecules in a volatile buffer (usually 0.05 M ammonium formate) and glycerol (30–50%) onto freshly-cleaved mica and shadowing with platinum in a vacuum evaporator (Denton Vacuum Co., Cherry Hill, NJ) (Weisel, et al., 1985). All of these specimens were examined in a Philips 400 electron microscope (Philips Electronic Instruments Co., Mahwah, NJ), usually operating at 80 kV and a magnification of 60,000×.

Scanning electron microscope experiments were carried out on clots that were fixed, dehydrated, critical point dried and sputter-coated with gold-palladium as described previously (Langer, et al., 1988). As much as possible, these clots were prepared for electron microscopy in the same way as the turbidity measurements were made; protein concentrations and buffer conditions were identical or similar. Samples for scanning electron microscopy were clotted for about 20× the gelation time in plexiglass microdialysis cells perforated for solvent perfusion. Specimens were washed 3× with pH 7.0 phosphate buffer to remove excess salt, fixed for 30 min in 2% glutaraldehyde, and rinsed 3×. Then, clots were poststained for 15 min with 1% osmium tetroxide, rinsed, and dehydrated in a series of ethanol concentrations up to 100%. The clots were critical point dried with CO_2 for ~45 min in a Denton apparatus (Denton Vacuum Co.), mounted and sputter coated with gold palladium. Specimens were examined in an Amray 1400 scanning electron microscope (Amray, Inc., Bedford, MA).

RESULTS

Model describing the kinetics of fibrin formation

Experimentally, clots have been characterized by the time course of turbidity development and electron micrographs of intermediates or final fiber structure. It has

8.2×10^{-6} M or 2.7 mg/mL), and there is an exponential decay as fibrinogen is converted to fibrin monomer. The rate of decay is dependent on the rate of cleavage of the A fibrinopeptides or the thrombin concentration. (*e*) The time dependence of the fibrin monomer concentration. The fibrin monomer concentration rises rapidly and then falls. The initial rise can be seen more easily in the expanded time scale of Fig. 2. (*f*) The average concentration of protofibrils that have not yet been incorporated into fibers as a function of time. There is a rapid rise followed by a slower decline. (*g*) Protofibrils incorporated into fibers as a function of time. There is a lag period, followed by a rapid rise in concentration which then approaches a maximum. (*h*) The average number of fibers as a function of time. There is a short lag period, a very rapid increase, quickly reaching a plateau. (*i*) The time course of the average fiber length. The maximum average length is quickly attained; the average length then remains constant or decreases slightly. An overshoot in length sometimes occurs under kinetic conditions where fibers of shorter length are formed at later times as fibrin monomer is depleted.

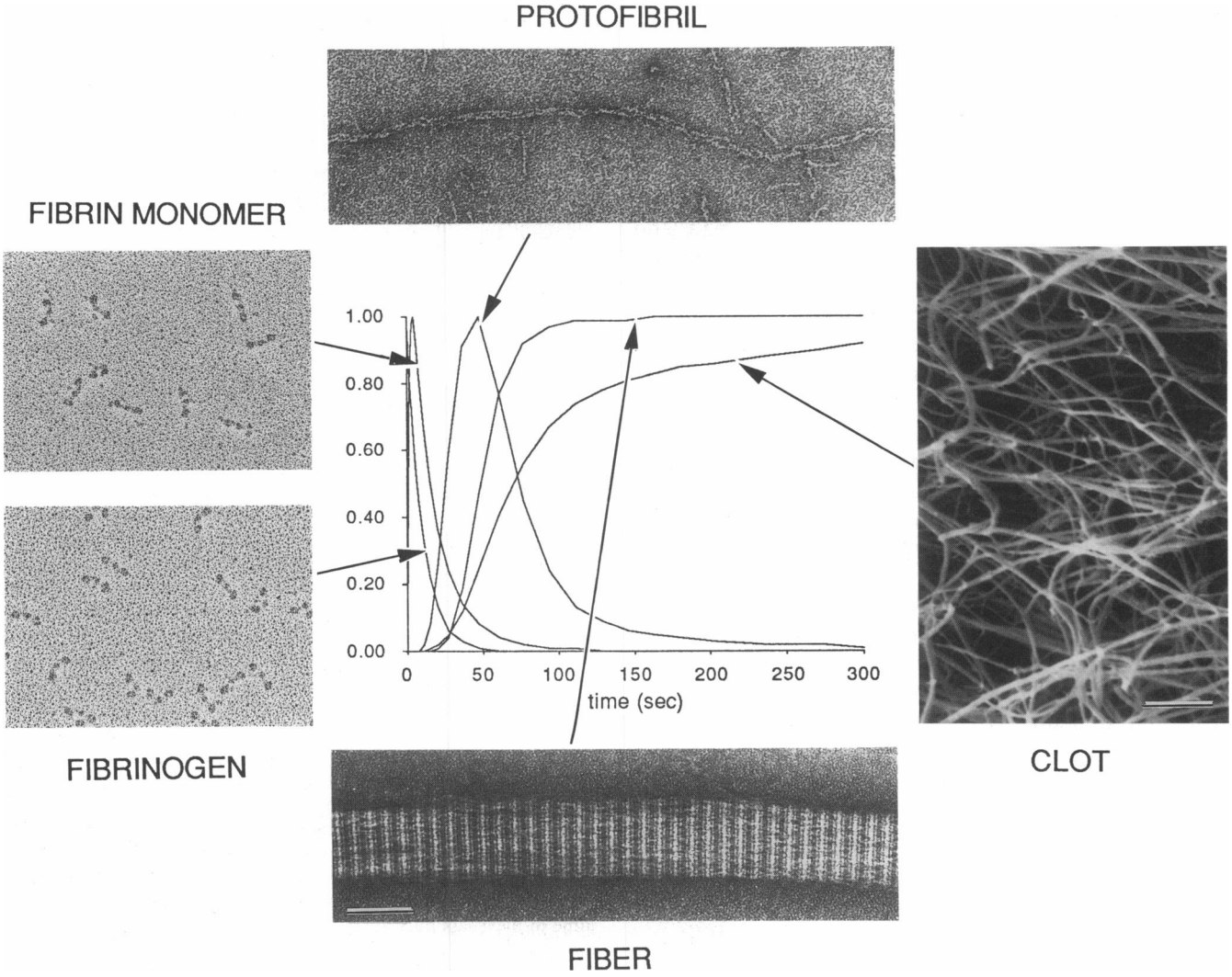

FIGURE 2 Electron microscopy correlated with kinetic modeling of some steps in fibrin polymerization. The kinetic modeling curves are the same as in Fig. 1, but the time scale is shorter to illustrate better the early events, and the values of various parameters have been normalized so that the time courses can be compared. The curves are identified by arrows from the electron micrographs associated with them. Fibrinogen and fibrin monomer molecules were both rotary shadowed with platinum; fibrin monomer was prepared in dilute acetic acid as described in the text. Samples of protofibrils formed during the lag period were prepared from fibrin monomer and negatively contrasted with uranyl acetate. Fibrin fibers produced just after the rapid rise in turbidity were also negatively stained. Images of individual molecules, protofibrils and the fiber are all shown at the same magnification; the bar represents 0.1 μm. The image of a clot is a scanning electron micrograph of a critical point dried specimen formed under roughly physiological conditions (0.15 M NaCl, 0.05 M Tris-HCl, pH 7.5). This clot image is a factor of 10 lower in magnification; the bar here represents 1.0 μm. The curve corresponding to the clot image is the average number of pf/fiber, which is directly related to turbidity as one measure of clot formation.

been demonstrated that the turbidity of clots is directly related to clot structure. Under most conditions, clot turbidity is proportional to the square of the average radius of the fibers (Carr and Hermans, 1978). Thus, turbidity is also proportional to the average number of protofibrils per fiber, assuming that fiber density is constant. Obviously, fiber diameters can be measured directly from electron micrographs. The average number of protofibrils per fiber has been calculated from kinetic models for direct comparison with experimental electron microscope and turbidity data.

The formation of a fibrin clot is commonly described as consisting of at least three steps: (*a*) the cleavage of the A fibrinopeptides by the enzyme thrombin; (*b*) association of fibrin monomers to form two-stranded protofibrils; and (*c*) aggregation of protofibrils to produce fibers which branch to yield a gel. Other steps and complications that arise from this simplified scheme will be discussed below. Aspects of the kinetics of the enzymatic reaction and subsequent molecular association have been studied (e.g., Janmey, et al., 1983; Lewis, et al., 1985; Wilf and Minton, 1986; Sato and Nakajima,

1984). Here, the kinetics of development of turbidity has been modeled, so these initial steps are oversimplified. We intentionally begin with a very simple model so that its limitations can be explored. The chemical reactions and their associated rate constants may be written as follows, where f_A represents fibrinogen, f is fibrin monomer, f_n is protofibrils and fr represents fibers:

$f_A \xrightarrow{k_A} f$ fibrinopeptide A cleavage to convert fibrinogen to fibrin

$f + f \xrightarrow{k_{pi}} f_n$ fibrin monomers associate, initiating protofibril formation

$f_n + f \xrightarrow{k_{pg}} f_n$ protofibrils grow in length

$f_n + f_n \xrightarrow{k_{fi}} fr$ two protofibrils aggregate to initiate a fiber

$fr + f_n \xrightarrow{k_{fg}} fr$ additional protofibrils add to a growing fiber.

Both aggregation steps, of fibrin monomers and of protofibrils, have been subdivided into initiation and growth reactions so that the sizes of the resulting structures can be modeled.

The differential equations describing the kinetics of these reactions are:

$$\frac{d[f_A]}{dt} = -k_A[f_A]$$

$$\frac{d[f]}{dt} = k_A[f_A] - 2k_{pi}[f][f] - k_{pg}[f][f_n]$$

$$\frac{d[f_n]}{dt} = k_{pi}[f][f] - 2k_{fi}[f_n][f_n] - k_{fg}[fr][f_n]$$

$$\frac{d[fr]}{dt} = k_{fi}[f_n][f_n].$$

In addition, if $[f_n^{tot}]$ = total protofibrils in fibers, then

$$\frac{d[f_n^{tot}]}{dt} = 2k_{fi}[f_n][f_n] + k_{fg}[fr][f_n]$$

and the average number of protofibril/fiber, $m = [f_n^{tot}]/[fr]$.

Using these relationships, and number average concentrations and rate constants based on those in the literature (e.g., Hantgan and Hermans, 1979; Lewis, et al., 1985; Wilf and Minton, 1986; Smith, 1984; note that all of the particular rate constants used for each experiment shown are given in the figure legends), the differential equations were solved numerically using an explicit Runge-Kutta method. The average number of protofibrils per fiber was calculated as a function of time (Fig. 1 *a*). Several features of typical experimental turbidity curves are observed. The average fiber size increases rapidly and then reaches a plateau. However, the average maximum number of protofibrils per fiber is very low. To simulate the real fiber diameters observed by electron microscopy or calculated from turbidity data, it was found to be necessary that addition of protofibrils to existing fibers be kinetically favored over initiation of new fibers by two protofibrils coming together. In other words, k_{fg} must be larger than k_{fi}. Under these conditions, a typical profile of turbidity is shown in Fig. 1 *b*. Note that there are no published values for k_{fi} and k_{fg}, but that the rates for association of protofibrils can be relatively fast even though the structures involved are large because an increase in target area would compensate for the decrease in diffusion rate for such large structures. In summary, with these rate constants, the observed average number of protofibrils per fiber is consistent with values determined experimentally from electron microscopy or turbidity data.

Alternatively, it may be that larger fibers are formed by the aggregation of smaller fibers, rather than simply adding protofibrils. This possibility was also modeled, simply by subtracting a term, $k_{fa}[fr][fr]$, where k_{fa} is the rate of fiber–fiber association, from the equation for the rate of change of the fiber concentration and adding the same term to the equation for the rate of change of total protofibrils in fibers. The average number of protofibrils per fiber can be increased in this way, but the curves are very different in shape than those in Fig. 1 *b*, where the values for fiber size reach a plateau, (i.e., the slope of the curves approaches zero). Instead, when fiber aggregation is sufficient to yield fibers with normal diameters and $k_{fg} = k_{fi}$, the slope of the curve for fiber size increases with time. Thus, fiber aggregation alone cannot account for both the shape of the curves and the magnitude of the final average fiber sizes reflected in the observed turbidity curves and electron micrographs.

The most serious problem with this model, however, is the failure to simulate the observed lag period. As might be expected, two of the rate constants particularly affect the initial portions of the curve, the rate of fibrinopeptide cleavage (k_A) and the rate of initial fibrin monomer association (k_{pi}). Decreasing either of these rate constants leads to a decrease in the maximal rate of fiber growth. Further decreases lead to the introduction of a lag period, but not before the shape of the curves has been seriously affected. At the point that a perceptible lag period appears, the slopes of the curves are greatly decreased and they rise slowly without reaching a plateau. In summary, it is not possible to simulate all observed features of the turbidity curves with such a simple model.[1]

[1] The relationship between turbidity and fiber size was developed for long fibers, i.e., those approaching the wavelength of light in length. To ensure that the lack of a lag period with this first model did not result

As shown by Hantgan and Hermans (1979), the lag period appears to be a result of the time necessary for protofibrils to grow to sufficient length before they aggregate. Such a requirement can be built into the model by defining the initial steps of protofibril formation explicitly and requiring that protofibrils reach a minimum length before they aggregate. The minimum length defined here is arbitrary; the minimum length actually employed in modeling can be based on experimental evidence, as described below.

$f_A \xrightarrow{k_A} f$ fibrinopeptide A cleavage to convert fibrinogen to fibrin

$f + f \xrightarrow{k_{pi}} f_2$ fibrin monomers associate to yield small oligomers, initiating protofibril formation

$f_2 + f \xrightarrow{k_{pi}} f_3$

$f_3 + f \xrightarrow{k_{pi}} f_4$

$\vdots$

$f_9 + f \xrightarrow{k_{pi}} f_{10}$

$f_{10} + f \xrightarrow{k_{pi}} f_n$ longer oligomers are formed, protofibrils capable of association

$f_n + f \xrightarrow{k_{pg}} f_n$ protofibrils grow in length

$f_n + f_n \xrightarrow{k_{fi}} fr$ two protofibrils aggregate to initiate a fiber

$fr + f_n \xrightarrow{k_{fg}} fr$ additional protofibrils add to a growing fiber.

The equations describing the kinetics of these reactions are:

$$\frac{d[f_A]}{dt} = -k_A[f_A]$$

$$\frac{d[f]}{dt} = k_A[f_A] - k_{pi}[f](2[f] + [f_2] + [f_3] + \cdots + [f_{10}]) - k_{pg}[f][f_n]$$

$$\frac{d[f_2]}{dt} = k_{pi}[f]([f] - [f_2])$$

$$\frac{d[f_3]}{dt} = k_{pi}[f]([f_2] - [f_3])$$

$$\vdots$$

$$\frac{d[f_{10}]}{dt} = k_{pi}[f]([f_9] - [f_{10}])$$

$$\frac{d[f_n]}{dt} = k_{pi}[f][f_{10}] - 2k_{fi}[f_n][f_n] - k_{fg}[fr][f_n]$$

$$\frac{d[fr]}{dt} = k_{fi}[f_n][f_n]$$

$$\frac{d[f_n^{tot}]}{dt} = 2k_{fi}[f_n][f_n] + k_{fg}[fr][f_n]$$

where $[f_n^{tot}]$ = total protofibrils in fibers;

$$\frac{d[c_{fn}]}{dt} = 11k_{pi}[f][f_{10}] + k_{pg}[f_n][f] - 2k_{fi}[f_n][c_{fn}] - k_{fg}[fr][c_{fn}]$$

where $[c_{fn}]$ = total fibrin in protofibrils;

$$\frac{d[c_{fr}]}{dt} = 2k_{fi}[f_n][c_{fn}] + k_{fg}[fr][c_{fn}]$$

where $[c_{fr}]$ = total fibrin in fibers;

average number fibrin/protofibril: $n = \frac{[c_{fn}]}{[f_n]}$;

average number protofibril/fiber: $m = \frac{[f_n^{tot}]}{[fr]}$;

average length of fibers: $l = \frac{[c_{fr}]}{[f_n^{tot}]}$.

In addition, small oligomers can also associate to form larger oligomers in a variety of ways. For example, $f_2 + f_n \rightarrow f_n$ and $f_2 + f_2 \rightarrow f_4$, et cetera. It is necessary to include some of these reactions. Without any oligomer–oligomer reactions, oligomers accumulate, slowing protofibril and fiber growth and producing normal lag periods but a very slow rise in turbidity. We modeled many permutations of such oligomer–oligomer reactions, with the result that there are usually only small differences in the protofibril/fiber curves with variations of which particular reactions are included. On the other hand, there can be great differences in the curves of some intermediates. Some of these differences may be important for understanding mechanisms of assembly, but do not seem to affect the simulated turbidity curves greatly. As more and more of these reactions are included, the effects become increasingly subtle, if they are noticeable at all. Thus, it appears to be unnecessary to include all permutations, although this conclusion was not tested because the computations become prohibitively time consuming.

from the oversimplification of ignoring the effects of shorter fibers at early times, we can assume that short fibers do not contribute to turbidity. (This assumption is probably not valid but is one most likely to produce a lag period.) Then, if we plot the average number of protofibrils per fibers that are at least 15 monomers long (which is ~350 nm, the wavelength of light used to measure turbidity), there is still no lag period. This result may be understood qualitatively by examination of Fig. 1*i*, which shows that fiber size rises very rapidly. Note that this oversimplification does not even need to be considered for all of the subsequent modeling because of the condition that oligomers reach a certain minimum length before they can aggregate to form fibers.

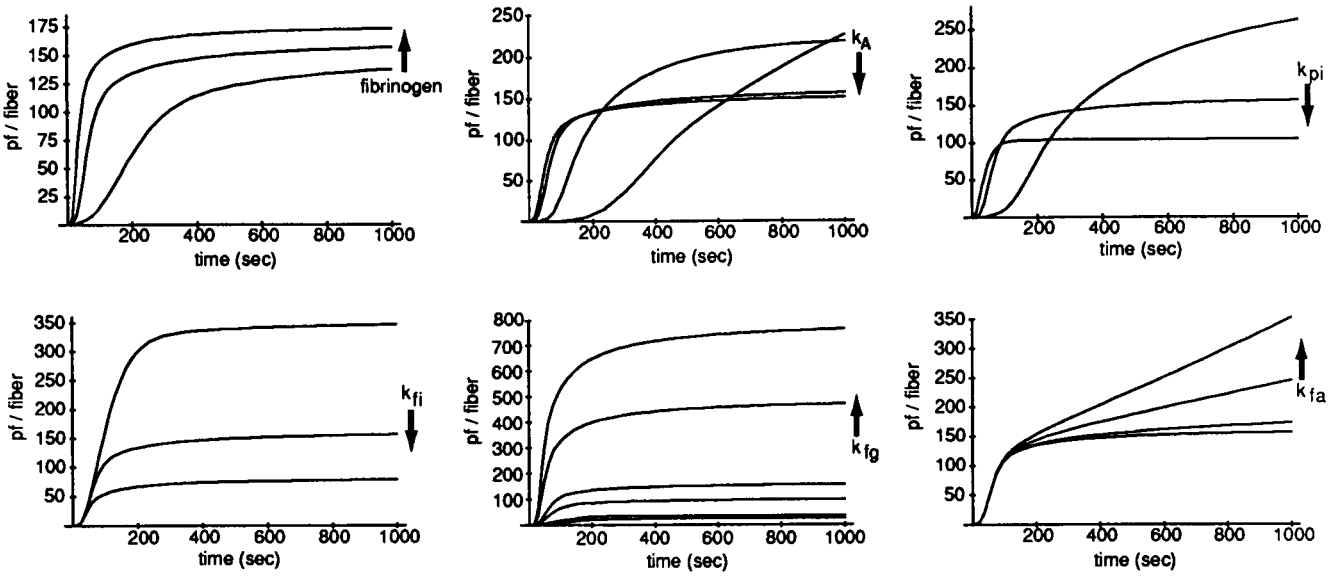

FIGURE 3 Kinetic modeling of the effects of changes in various rate constants on turbidity curves. The average number of protofibrils per fiber is plotted as a function of time. In each set of curves, one parameter is varied while all others are held constant; the parameter that is changed is shown to the right of the curves, with the arrows indicating the curves corresponding to an increase in that parameter. The changes in the computed curves may be compared with the observed turbidity curves of later figures and in other studies. See also Table 1.

These equations and those resulting from a variety of other possibilities of aggregation of oligomers were solved. Because the basic results of all of these models were similar, although details differed, some of these oligomer reactions were included in all subsequent modeling. In all models featuring a requirement that protofibrils reach a minimum length before lateral aggregation, the curve of protofibrils per fiber versus time shows a distinct lag period (Fig. 1 *c*). It should be noted that the actual kinetic parameters are not known in any detail, so the shape and general features are more significant than the actual numerical values. Rate constants have been chosen to be consistent with known values and to give curves that resemble those observed.

The average maximum values for number of protofibrils per fiber are close to those determined experimentally (Voter, et al., 1986; Weisel and White, unpublished observations). As discussed above, to obtain this result, it was found to be necessary that addition of protofibrils to existing fibers be kinetically favored over initiation of new fibers by two protofibrils coming together, i.e., k_{fg} must be larger than k_{fi}. If we assume that protofibril aggregation is cooperative, i.e., big protofibrils grow faster than small ones, we must add additional reactions such that rates of adding subsequent protofibrils to a growing fiber increase. The effect of this modification is to yield curves where there is a higher maximal rate followed by a gradual rise rather than a plateau, leading to thicker fibers.

The length of the lag period in the model varies with the number of monomers added to the protofibril before it can associate with another protofibril. Experimentally,

TABLE 1 Effects on clot structure and assembly of changes in parameters as determined from kinetic modeling

	Results in an increase (↑) or decrease (↓) in				
Increase in the rate constant	Maximum fiber size	Maximum rate of assembly	Lag period	Number of fibers	Fiber length
k_A - FPA cleavage	↓	↑	↓	↑	↓
k_{pi} - pf initiation	↓	↑	↓	↑	↑
k_{pg} - pf growth	0	0	0	0	↑
k_{fi} - fiber initiation	↓	↓	0	↑	↓
k_{fg} - fiber growth	↑	↑	↓	↓	↓
k_{fa} - fiber aggregation	↑	0	0	↓	↓
or fibrinogen conc.	↑	↑	↓	↑	↑

Abbreviations: FPA = fibrinopeptide A; pf = protofibril.

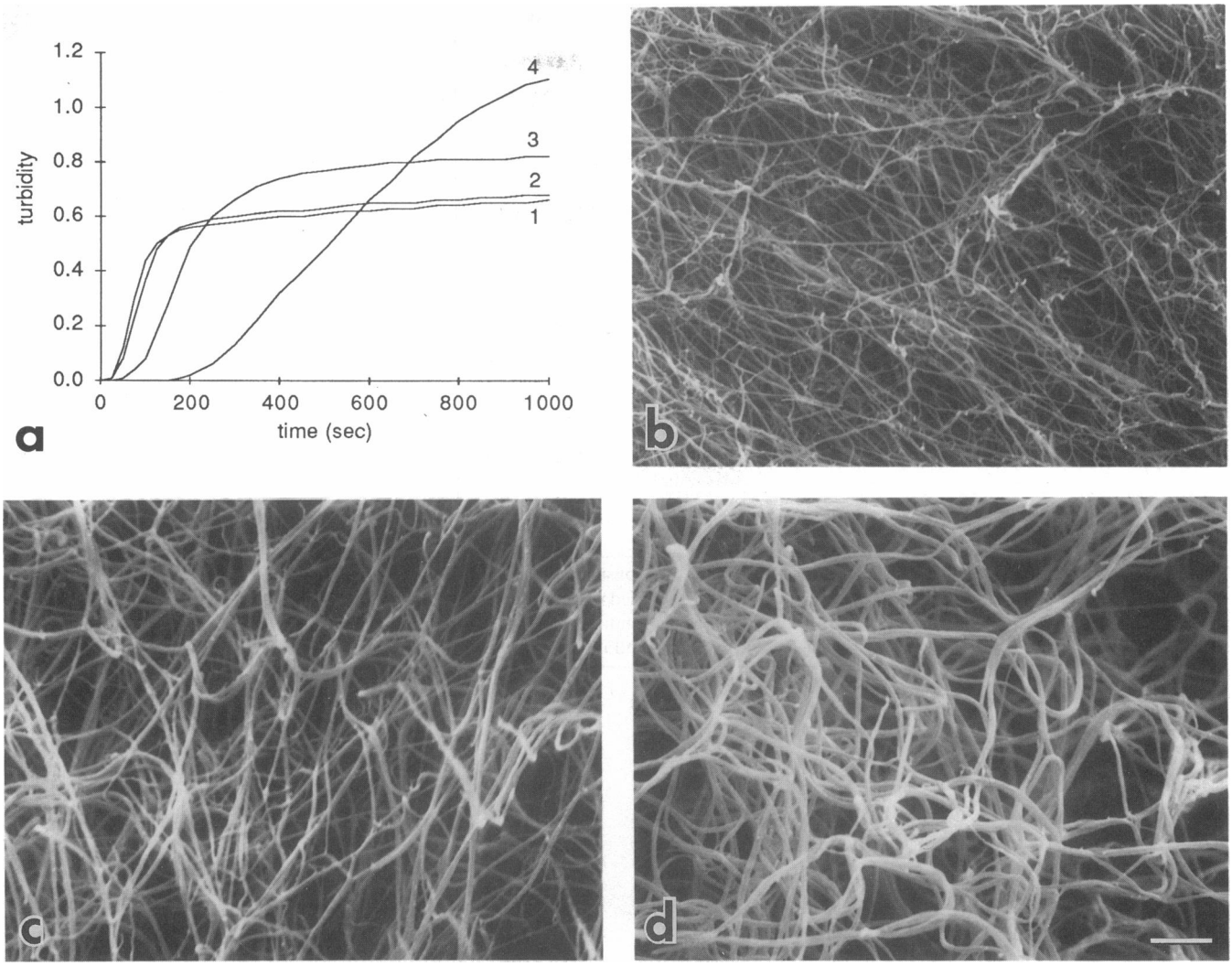

FIGURE 4 Effects of thrombin concentration on clot structure and turbidity curves. (*a*) Turbidity curves for clots formed using different thrombin concentrations: (1) 1 unit/mL; (2) 0.1 unit/mL; (3) 0.01 unit/mL; (4) 0.001 unit/mL. Compare these curves with the variation of k_A in Fig. 3. (*b*, *c*, and *d*) Scanning electron micrographs of clots formed using different concentrations of thrombin: (*b*) 1 unit/mL; (*c*) 0.01 unit/mL; (*d*) 0.001 unit/mL. The bar represents 1.0 μm.

the lag period varies with the conditions of clotting. For the lag period of the model to correspond to that of clots formed under approximately physiological conditions, it was determined that a protofibril must consist of 10–20 monomers. This is very similar to the lengths of protofibrils observed (Hantgan, et al., 1980; Medved, et al., 1990) and the values calculated from light scattering data (Hantgan and Hermans, 1979).

A model in which the A fibrinopeptides are removed sequentially was also tested, because this question is still controversial. Because this modification introduces many more possible reactions, the complexity increases greatly. Therefore, the results depend on the assumptions made, although for most of the rates of fibrinopeptide cleavage used for the modeling here, there are no significant effects on the protofibril/fiber curves. At slower rates of cleavage, this modification can have effects on the initial portions of the curves, including the lag period and rate of fiber growth.

The concentrations of all of the intermediates in clot formation can also be calculated for any particular kinetic parameters. The fibrinogen concentration falls exponentially, with a rate dependent on k_A (Fig. 1 *d*). Fibrin monomer concentration rises rapidly and then falls at a rate dependent in a complex way on its incorporation into small oligomers and protofibrils (Fig. 1 *e*; note that the rise is more visible with the shorter time scale of Fig. 2). The concentration of free protofibrils, or those not incorporated into fibers, rises after a lag period and then declines as the protofibrils aggregate (Fig. 1 *f*). The concentration of protofibrils in fibers increases rapidly after a lag period and then levels off as protofibril forma-

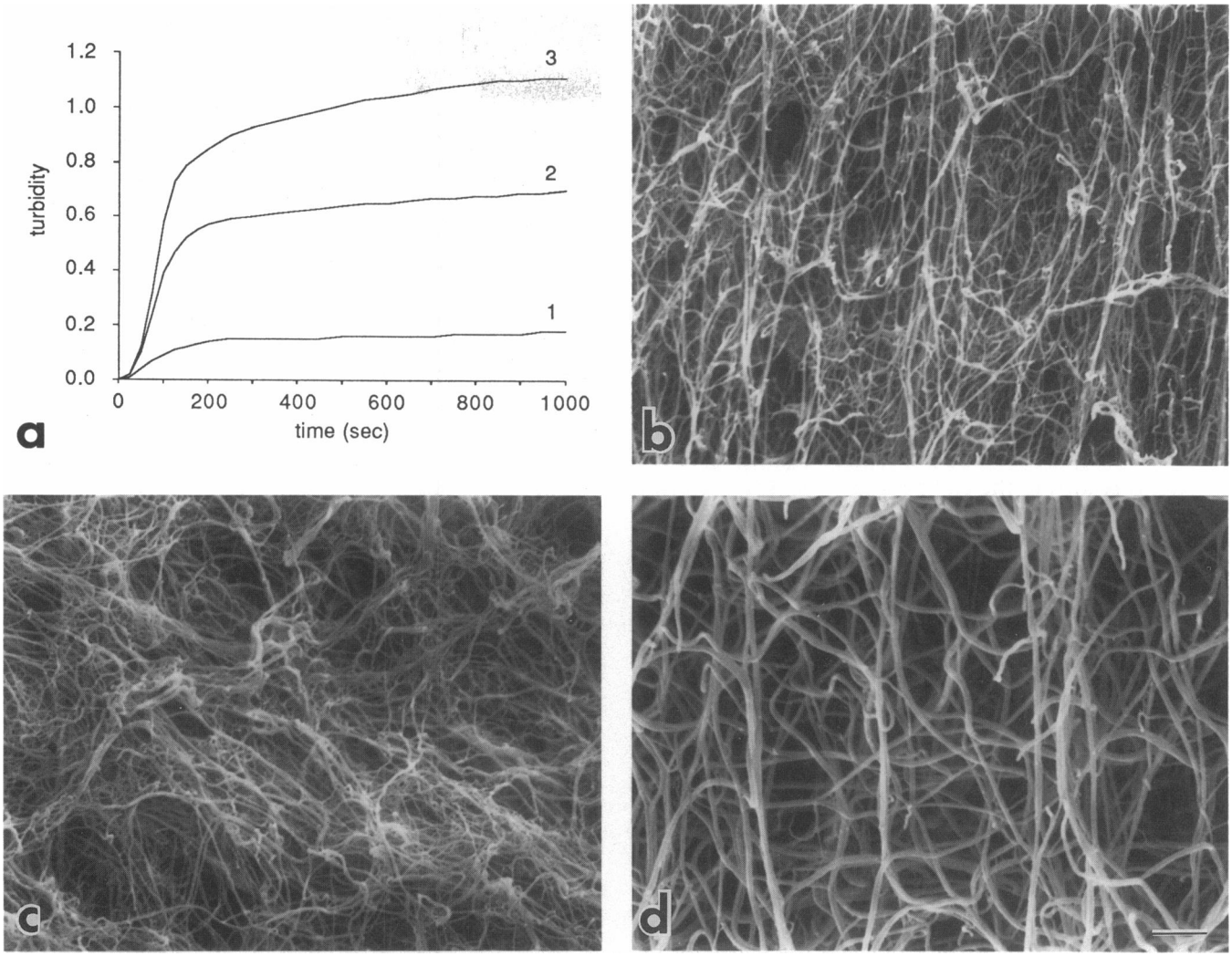

FIGURE 5 Effects of salt concentration on clot structure and turbidity curves. (*a*) Turbidity curves for clots produced in different salt concentrations: (1) 0.4 M NaCl; (2) 0.15 M NaCl; (3) 0.05 M NaCl. Compare these curves with the variation of k_{fg} in Fig. 3. (*b*, *c*, and *d*) Scanning electron micrographs of clots formed in different concentrations of salt: (*b*) 0.15 M NaCl; (*c*) 0.4 M NaCl; (*d*) 0.05 M NaCl. The bar represents 1.0 μm.

tion ceases when fibrin monomers are used up (Fig. 1 *g*). The curve for fiber concentration has a similar shape, but rises more rapidly and reaches a plateau at a lower value (Fig. 1 *g*).

The average length of fibers with time can also be calculated (Fig. 1 *h*). It is important to note that protofibrils may grow in length even after they are incorporated into fibers, a necessary requirement of any realistic model. Even though the lengths are affected by several of the rate constants and other aspects of the kinetic modeling, it was discovered that it is difficult to obtain long protofibrils or fibers unless k_{pg} is greater than k_{pi}. Although actual fiber lengths cannot be measured easily, it is apparent from electron micrographs of clots that fibers are very long. Because we do not know accurately the lengths of protofibrils and fibers, the difference between these two rate constants in the examples here is somewhat arbitrarily chosen. However, it does appear that protofibril elongation must be preferred over the initial association of monomers to yield a long protofibril.

The various intermediates in clot formation have also been examined by electron microscopy. Examples of these structures are shown in Fig. 2, together with the time courses of the computed concentrations of the intermediates. All of the curves have been normalized so that they can be shown on the same scales for comparison of the time courses. Rotary shadowed individual fibrinogen molecules are 45-nm long and have a characteristic trinodular shape, with the subdivision of the end regions apparent in some images (Erickson and Fowler, 1983; Weisel, et al., 1985). Fibrin monomer molecules were observed by electron microscopy in preparations at very early stages of clot formation, as suggested by these curves. Fibrin monomers, obtained by dissolving clots at

pH 3.5, appear to be generally similar to fibrinogen, suggesting that there are no large-scale conformational changes upon cleavage of the fibrinopeptides. Many protofibrils were observed from electron microscope preparations during the lag period, in agreement with these curves. Negatively contrasted protofibrils are made up of molecules half-staggered to yield two filaments of molecules bonded end-to-end and twisting around each other (Fowler, et al., 1981; Medved', et al., 1990). Fibers appear somewhat later and are best observed before gelation of the clot. The fibrin fiber is a paracrystalline structure with a repeat of 22.5 nm, or half of the molecular length, as a result of the half-staggered arrangement of molecules; the band pattern has been related directly to the molecular structure and packing (Weisel, 1986*a*). The curve of protofibrils per fiber, corresponding to turbidity, is related to the clot structure, as illustrated by a scanning electron micrograph, at lower magnification than the other micrographs, showing fiber bundles that aggregate and branch to form a gel.

Kinetic modeling of the effects of changes in the rates of fibrinopeptide cleavage, protofibril formation and lateral aggregation

With the establishment of this basic scheme for the steps of fibrin assembly, the effects of various changes in rate constants or other factors can be investigated. Some of these effects are shown in Fig. 3 The average number of protofibrils per fiber, or turbidity, is plotted versus time. In each case, one parameter has been varied, keeping all others constant. The arrows indicate the effects of increasing each parameter. Table 1 also summarizes some of these conclusions, the effects on average maximum fiber size, maximum rate of assembly and lag period, in addition to the effects on other characteristics, such as the average fiber length and number of fibers. It should be noted that many of these effects are observed only within a certain range of values for the rate constants.

Increasing the fibrinogen concentration leads to a decrease in the lag period, an increase in the maximum rate of change and an increase in the maximum final fiber size (Fig. 3). The number of fibers and their lengths also increase. Experimental results show similar changes, although it should be noted that, similar to the effects of salt concentration, opposite effects can occur at higher fibrinogen concentrations (Ferry and Morrison, 1947). The effects of changes in k_A, the rate of fibrinopeptide A cleavage, are more complex (Fig. 3). Increasing this rate constant results in a decrease in the lag period, an increase in the maximum rate of fiber growth and a decrease in final fiber size. The number of fibers in the final clot increase, while their average length decreases. The effects of increasing k_{pi}, the rate of initiation of protofibril formation, are generally similar, although the magnitude of some of the changes is considerably different (Fig. 3). The lag period decreases, the maximum rate of assembly increases, and the final size decreases, while both the number of fibers and their lengths increase. The only effect of increasing k_{pg}, the rate of protofibril growth, is to increase the final length of the protofibrils and hence the fibers, so these changes have not been included in Fig. 3. Increasing k_{fi}, the rate of initiation of fiber formation, decreases final fiber size, with little change in lag period or maximum rate of growth; at the same time, the number of fibers increase greatly and fiber length decreases slightly (Fig. 3). As k_{fg}, the rate constant for addition of protofibrils to fibers, increases the lag period decreases, the maximum rate of assembly increases and the final size increases (Fig. 3). Fewer fibers are formed and they are shorter. Finally, the effects of aggregation of preformed fibers to yield thicker fiber bundles (Weisel, 1986*b*) was also added to the equations (Fig. 3). There is little effect on the initial portion of the curve, but, rather than leveling off, the fiber size continues to increase. As a result there are fewer fibers and they are somewhat shorter.

Experimental observations on variations in clot structure: turbidity and electron microscopy

The effects of several different types of changes in environmental conditions were measured by monitoring the changes in turbidity over time and examining the resulting clots by scanning electron microscopy. The effects of changes in thrombin concentration and ionic strength, as well as the influence of the addition of small amounts of thrombospondin or platelet factor 4, were determined. In addition, the effects of some other changes described in the literature will be evaluated in the Discussion.

The effects of thrombin concentration on turbidity development are well known. If the thrombin concentration is high, changes in its concentration have no effect. With lower amounts of thrombin, increasing the thrombin concentration causes a decrease in the lag period, an increase in the maximum rate of turbidity development and a decrease in the maximum final turbidity (Fig. 4 *a*). Electron micrographs of clots formed with three different thrombin concentrations are also shown in Fig. 4, *b–d*. Consistent with the turbidity differences, increasing thrombin results in more fiber bundles that are thinner. As thrombin concentration is decreased, the average fiber bundle size and lag period increases, while the maximum rate of turbidity development decreases.

The effects of ionic strength have also been extensively studied in many laboratories. With an increase in ionic

strength, the lag period increases, the maximum rate and the maximum turbidity decrease (Fig. 5 *a*). Observation of clots by scanning electron microscopy indicates that, as ionic strength increases, the number of fiber bundles increases, but their diameters decrease (Fig. 5, *b–d*). The average size of the pores between fiber bundles also decreases.

Small amounts of thrombospondin cause striking changes in the structure of clots (Bale and Mosher, 1986). These changes are especially noticeable at low concentrations of thrombin. Under these conditions, thrombospondin causes a decrease in the lag period and in the final maximum turbidity and an increase in the number of fibers (Fig. 6, *a*). Because such conditions are not represented in the calculated curves of Fig. 3, these turbidity curves were simulated by calculation of fiber size at low thrombin concentration with changes in various rate constants that could be affected by thrombospondin. The only changes resembling those observed arise from an increase in k_{fi}, the rate of initiation of fiber formation (Fig. 6 *b*). In addition, the size of the protofibrils before lateral aggregation was decreased to simulate the observed decrease in the lag period; such changes would be consistent with an increase in k_{fi}, as discussed below. Scanning electron micrographs corresponding to the addition of thrombospondin are shown for two different concentrations of thrombin (Fig. 6, *c–f*).

Very low concentrations of platelet factor 4 cause changes in turbidity of fibrin clots (Carr, et al., 1987). There is little change in the beginning portions of the curves, but final turbidities are significantly larger and the maximum turbidity continues to rise slowly, rather than leveling off, as it normally does (Fig. 7, *a*). These effects are reflected in the electron micrographs of clots with increasing amounts of platelet factor 4 (Fig. 7, *b–d*), which show thicker fiber bundles with larger pores.

DISCUSSION

Suggestions on the mechanism of fibrin polymerization from kinetic modeling

Using information about the chemical reactions involved in fibrin polymerization, equations describing the kinetics of assembly can be written and then solved numerically. The results can be related to many experimental observations. Initially, calculated curves of the number of protofibrils per fiber over time can be compared to measured turbidity profiles. A simple model, consisting of fibrinopeptide cleavage, protofibril formation and lateral aggregation to produce fibers, yields curves indicating that the average fiber size increases rapidly and then levels out. The observed lag period can be simulated by requiring that oligomers reach a certain minimum length before they can aggregate, a characteristic of nucleation polymerization rather than condensation polymerization. Although this conclusion is in agreement with experimental observations (Hantgan and Hermans, 1979), the kinetic modeling here suggests that the requirement of a minimum protofibril length for lateral aggregation is not just a result of the relative rates of protofibril growth versus lateral aggregation. Instead, lateral aggregation may require the cumulative effect of many weak interactions along protofibrils of sufficient length. The average size of protofibrils determined from modeling of the lag period is in good agreement with electron microscope observations. This reaction scheme can account for most experimental observations of the effects of a variety of factors that influence fibrin assembly.

Rate constants for the initial steps of this scheme have been determined elsewhere and values used in the simulations were similar. Where rate constants were not known, appropriate values were adjusted to yield curves of changes in fiber size similar to observed turbidity curves and electron microscope observations. During this process, it was found that, to simulate that fiber diameters observed by electron microscopy or calculated from turbidity or light scattering data, the addition of protofibrils to existing fibers must be kinetically favored over the initiation of new fibers by two protofibrils coming together. In other words, addition is faster than initiation. These results suggest that there may be some cooperativity in the aggregation of protofibrils.

Similarly, calculation of the lengths of protofibrils and fibers suggests that the growth of protofibrils may be favored over initiation of protofibrils; otherwise, the computed average fiber lengths are more limited than might be expected. This result, however, is tentative for several reasons, and it is clear that more experimental data are needed to resolve this question. The lengths of fibers cannot generally be measured from electron micrographs because it is difficult to discern the ends of fibers and to trace an individual fiber. Most importantly, such a result appears to contradict experimental evidence that monomer–monomer association is the same as monomer-oligomer or oligomer–oligomer association (Hantgan and Hermans, 1979). Finally, this aspect of the simulations is dependent on the extent to which various types of oligomer-oligomer associations are significant. Although this is still unknown, the modeling has demonstrated that oligomer–oligomer associations are essential to produce curves similar to the experimental turbidity curves.

The kinetic model described here is based on mechanisms developed from basic evidence and is also consistent with most other experimental studies of assembly. The initial model has been oversimplified for two rea-

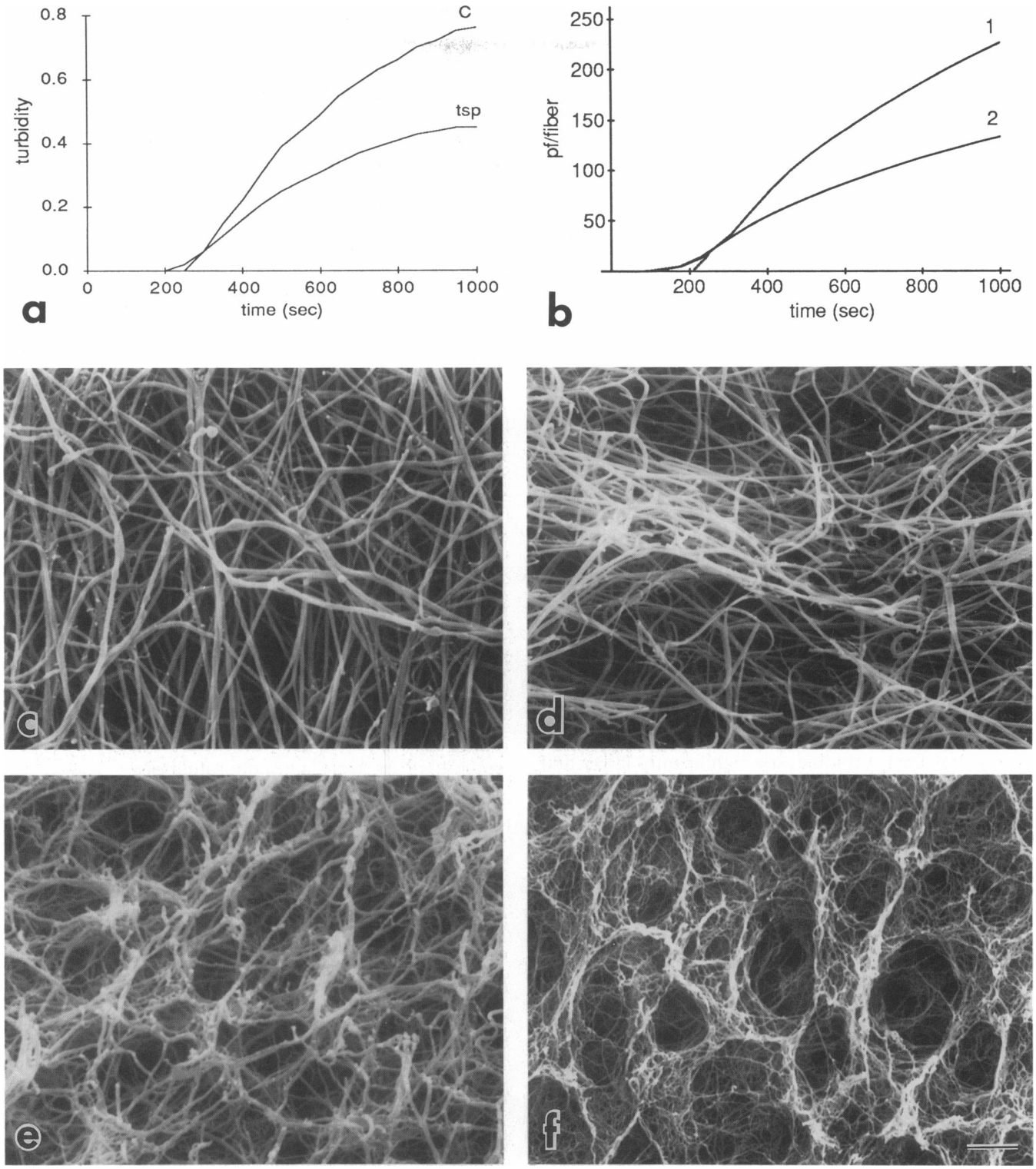

FIGURE 6 Effects of thrombospondin on clot structure and turbidity curves. (*a*) Turbidity curves for 0.01 units/mL thrombin and 0.3 mg/mL fibrinogen, with and without added thrombospondin: *C* = control, no thrombospondin; tsp = thrombospondin, same conditions as the control with the addition of 40 μg/mL thrombospondin. (*b*) Modeling of the turbidity curves in (*a*); fibrinogen concentration = 5×10^{18} molecules/L; $k_A = 10^{-3}\ s^{-1}$. (1) $k_{fi} = 10^{-21}$ L/molecule s; $k_{fg} = 2 \times 10^{-17}$ L/molecule s; (2) $k_{fi} = 10^{-20}$ L/molecule s; $k_{fg} = 2.4 \times 10^{-17}$ L/molecule s (*c*, *d*, *e*, and *f*) Scanning electron micrographs of clots with and without thrombospondin: (*c*) control, 0.3 mg/mL fibrinogen, 0.002 units/mL thrombin; (*d*) same conditions with 40 μg/mL thrombospondin; (*e*) control, 0.3 mg/mL fibrinogen, 0.01 units/mL thrombin; (*f*) same conditions with 40 μg/mL thrombospondin. The bar represents 1.0 μm.

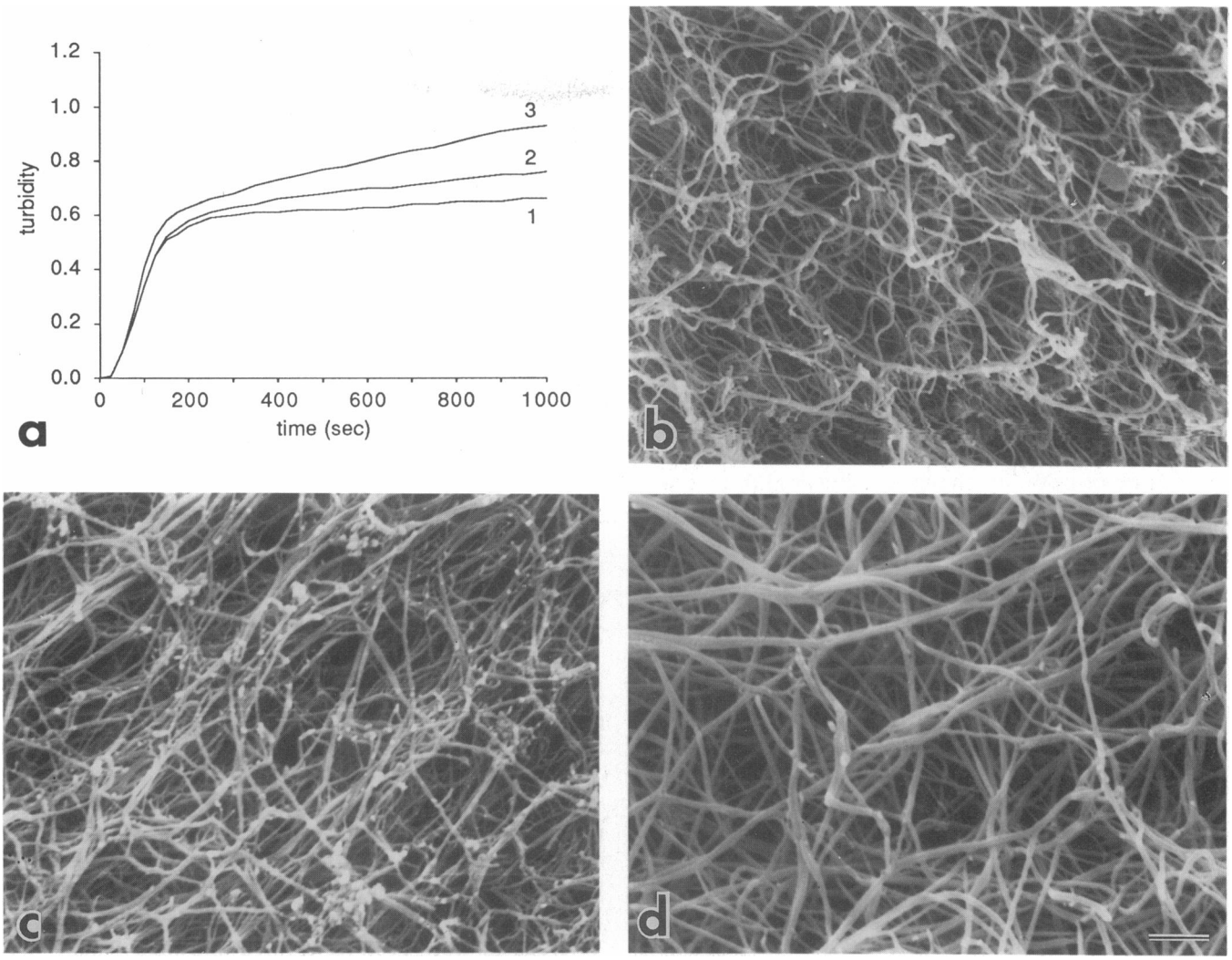

FIGURE 7 Effects of platelet factor 4 on clot structure and turbidity curves. (*a*) Turbidity curves showing the effects of addition of platelet factor 4: (1) control, no platelet factor 4; (2) same conditions as the control with the addition of 5 ng/mL platelet factor 4; (3) 10 ng/mL platelet factor 4. Compare these curves with the variation of k_{fa} in Fig. 3 (*b*, *c*, and *d*) Scanning electron micrographs of clots with and without platelet factor 4: (*b*) control, no platelet factor 4; (*c*) same conditions with 5 ng/mL platelet factor 4; (*d*) 1,000 ng/mL platelet factor 4. The bar represents 1.0 μm.

sons. Even such a simplified model rapidly becomes difficult to solve mathematically. More importantly, simplification is necessary to sort out the significance of various proposed mechanisms. This type of modeling is important for generating hypotheses than can be tested, as illustrated in the last paragraph. In whatever ways the current model fails, it can be modified so that its behavior corresponds more closely to observations. Fibrin assembly is a very complex system whose behavior cannot always be predicted intuitively. For example, the interplay between average fiber diameter and length and number of fibers directly affects turbidity but can be very complicated for such a multistep mechanism. Furthermore, this kinetic modeling provides a framework for thinking about and analyzing the effects of various modifications to the basic scheme.

Conclusions about fibrin assembly from correlation of kinetic modeling and structural data

Fibrinopeptide cleavage

The model described here successfully predicts the effects of changes in the rate of fibrinopeptide cleavage and fibrinogen concentration on fiber bundle size (Fig. 3 and Table 1). Experimental curves for thrombin cleavage are illustrated in Fig. 4; the turbidity curves for different concentrations of batroxobin, which specifically cleaves the A fibrinopeptides, were also measured (data not shown), and, as demonstrated by others (e.g., Shen, et al., 1977; Carr, et al., 1985; Pirkle, et al., 1986), they are qualitatively similar to those for thrombin and can be fit by the kinetic model here. Both experimental and model

data show that at low enzyme concentrations, or slow rates of cleavage, the maximum rate of growth of fibers is slow and the maximum turbidity or fiber size is large. This result can be described in words as follows: at low thrombin concentrations, fibrinopeptide cleavage is slower so that protofibrils are formed more slowly, and shorter protofibrils aggregate as they are formed, resulting in thicker fibers. On the other hand, at higher enzyme concentrations, the maximum rate of assembly is greater and the maximum turbidity is lower. In other words, here fibrinopeptide cleavage and protofibril formation are rapid compared to lateral aggregation, so long thin protofibrils are formed before they can aggregate with each other. Aspects of the experimental curves resulting from different enzyme concentrations have been studied. Plots of maximum turbidity versus maximum rate of turbidity change are linear (Pirkle, et al., 1986); plots derived from the calculated curves are similar. Results from some abnormal fibrinogens where the rate of cleavage of the A fibrinopeptides is affected may also be accounted for by this model.

Cleavage of fibrinopeptide B generally follows that of A temporally and occurs more readily after protofibril and fiber assembly. The effects of fibrinopeptide B cleavage were not directly modeled here, but most of the effects can be simulated by changes in k_{fg}. Such changes in lateral aggregation would be expected considering the measured increase in calcium binding accompanying fibrinopeptide B cleavage (Mihalyi, 1988). For example, cleavage of fibrinopeptide B, like an increase in k_{fg}, can result in a decrease in the lag period, an increase in the maximum rate of turbidity development and an increase in the maximum turbidity (Shen, et al., 1977; Pirkle, et al., 1986). Likewise, larger fiber bundles are observed by electron microscopy upon cleavage of fibrinopeptide B (Weisel, 1986*b*; Mosesson, et al., 1987). It should be noted, however, that the effects of fibrinopeptide B cleavage can differ from these results because they depend on the exact experimental conditions (Pirkle, et al., 1986; Carr, et al., 1985). It should also be mentioned that experimental results under various conditions where thrombin is used for clot formation (e.g., results section above) can be simulated by this model qualitatively even though only fibrinopeptide A removal is explicitly considered, because most aspects of fibrinopeptide B cleavage can be accounted for simply by variation of k_{fg}, and hence the curves are similar whether one or both pairs of peptides are cleaved.

Effects of various factors on lateral aggregation

A great many studies have linked changes in the chemical environment of the clot with influences on lateral aggregation, usually by measurements of turbidity over time. For example, the effects of salt concentration and pH are well known (Ferry and Morrison, 1947; Latallo, et al., 1962; Müller, et al., 1981; Carr, et al., 1985). Calcium ions are one of the most potent modulators of clot structure. Most of the time, the description of observations in terms of changes that affect lateral aggregation has been used somewhat loosely, usually meaning only that the maximum turbidity or average fiber size was increased over that under physiological conditions. However, it is clear from Fig. 3 and Table 1 that there are several very different mechanisms that would all result in higher turbidity or fiber size. For example, decreasing the rates of fibrinopeptide cleavage or fibrin monomer aggregation or fiber initiation all result in larger fiber bundles. Here we would like to use lateral aggregation to mean the addition of protofibrils to a growing fiber. In investigating the mechanisms and binding sites involved in lateral aggregation, it is important not to be misled by the many factors that affect various rates of assembly and hence turbidity or average sizes of fiber bundles. For example, the fact that proteolytic removal of a part of the fibrinogen molecule leads to thinner fibers does not imply that the portion removed comprises any binding sites for lateral aggregation.

An increase in the rate of lateral aggregation, or addition of protofibrils to a fiber, corresponds to an increase in k_{fg}. From Table 1, it may be observed that kinetic modeling suggests that an increase in lateral aggregation commonly results in an increase in the maximal rate of assembly, a decrease in the lag period, the number of fibers and the fiber length, as well as an increase in the maximum average fiber size. Many of these parameters have been observed in various studies in the past, but some are more difficult to determine than others. The average number of fibers formed and their lengths are very difficult to measure. Of course, the maximum fiber size, rate of assembly and lag period can be determined directly from the turbidity curves, with the provisos mentioned above. On the other hand, not all publications on this topic show turbidity curves directly; some include only maximum turbidity, for example. It is possible, then, to propose that some phenomena described in the literature result from effects on lateral aggregation in this strict sense, although in many cases not enough information is available. In most cases, the maximum turbidity and maximum rate of turbidity development are increased and the lag period is decreased.

A basic concern is that it is unlikely that many of these environmental factors have effects only on lateral aggregation. For example, changes in salt concentration or pH will affect the charges of proteins and hence the intermolecular interactions of all components. Some of these interactions include the binding of thrombin to fibrinogen, the release of cleaved fibrinopeptides, the interaction of fibrin monomer to form small oligomers and protofibrils, all interactions of protofibrils with each other and with fibers, and fiber/fiber interactions. The overall

effect will depend on the relative magnitudes of all of these individual interactions. The effects of proteins and some other compounds are probably more likely to be specific in their effects on particular steps of the polymerization process.

Thrombospondin affects protofibril association

Several proteins released by activated platelets have effects on fibrin clot formation. Thrombospondin is a protein, with a molecular mass of 450 kD made up of three identical polypeptide chains, that accounts for ~25% of the protein secreted from platelet α granules. This protein interacts specifically with fibrinogen as well as a few other clotting proteins and several roles for it in hemostasis and cell adhesion have been proposed (Tuszynski, et al., 1987). In fibrin formation, small concentrations of thrombospondin reduce the lag period and the maximum turbidity. The effects of thrombospondin appear to be unique in that both the lag period and the maximum turbidity are decreased. Scanning electron microscopy of clots in the presence of thrombospondin reveal a corresponding increase in the number of fiber bundles but they are thinner. The results presented here are in general agreement with previous observations, although in earlier studies the absorbance was measured at a different wavelength and samples were prepared for transmission electron microscopy using a high voltage instrument (Bale and Mosher, 1986).

Bale and Mosher (1986) presented a thorough analysis of the interpretation of their results. Even though it has been demonstrated that thrombin and thrombospondin can form a covalent complex, it seems unlikely that the observed effects on clot structure arise from any effect on thrombin or fibrinopeptide cleavage. On the contrary, thrombospondin also interacts directly with fibrin, and it appears that fiber growth is affected by interactions with fibrin intermediates. The three polypeptide chains of thrombospondin could comprise three equivalent binding sites for fibrin and may serve as a trifunctional branch point for fibrin intermediates (Bale and Mosher, 1986).

Some of these suggestions can be analyzed using the kinetic model described here. Although branching is not explicitly included in the present kinetic model and so cannot be tested, the basic concept that thrombospondin can affect clot structure by specific interactions with fibrin oligomers can be. If, as suggested by Bale and Mosher (1986), thrombospondin can link fibrin oligomers and bring them together, the rate of initiation of fibers, k_{fi}, and, to a lesser extent, the rate of addition of protofibrils to fibers, k_{fg}, would be affected. In these experiments there were about nine fibrin molecules for each thrombospondin, so there would be about one thrombospondin for each 200 nm of protofibril. In addition, smaller oligomers might also be brought together so that the minimum protofibril size that can form aggregates would be decreased, resulting in a decrease in the lag period.

Because the most striking experimental effects are observed at low thrombin concentration, the effects of varying these rate constants on the calculated turbidity profiles were determined under the same conditions. In addition, the minimum protofibril size for lateral aggregation was decreased, also corresponding to the hypothesis described above. Model curves are in good agreement with experimental data in that both the lag period and the average maximum fiber size are decreased (Fig. 6). These results are consistent with the idea that thrombospondin may help to bring protofibrils together. Thus, shorter oligomers may aggregate, decreasing the lag period. Protofibrils would aggregate more readily, resulting in more thin protofibrils (Table 1). These results are similar to what was observed experimentally for thrombospondin. Note that the effects on fiber size of increasing k_{fi}, the rate of two protofibrils coming together to initiate a fiber, is opposite to that of increasing, k_{fg}, the rate of addition of protofibrils to a growing fiber (i.e., lateral aggregation).

Platelet factor 4 affects fiber aggregation

Platelet factor 4 is a cytokine with a molecular mass of 7.8 kD that is secreted from platelet α granules in a complex with a high molecular weight proteoglycan carrier (Holt and Niewiarowski, 1989). Platelet factor 4 causes a striking increase in turbidity and in the average diameter of fiber bundles as observed by electron microscopy (Fig. 7). The results presented here are similar to those reported previously (Carr et al., 1987). Even very low concentrations of platelet factor 4 have profound effects on turbidity curves. Although it might be expected that such a phenomenon would be mediated through influences on the enzymatic cleavage reaction, there does not appear to be any effect of platelet factor 4 on thrombin cleavage measured by the thrombin-S2238 assay (Carr, et al., 1987). The major effect on the turbidity curves is at later times; the turbidity continues to rise gradually instead of reaching a plateau quickly (Fig. 7 *a*; Carr et al., 1987). By varying the different parameters in the kinetic model here, it was demonstrated that curves similar to those observed can be generated by increasing the rate of aggregation of fibers to form larger fiber bundles, k_{fa} (see Fig. 3 and Table 1). In other words, the increases in turbidity caused by platelet factor 4 may be accounted for by aggregation of fibers to yield larger bundles. The effects of platelet factor 4 are observed even at molar ratios of fibrin:platelet factor 4 as high as 10,000:1. The mechanism proposed here could account for this very low concentration of platelet factor 4 necessary for observation of these effects, because even a low ratio of platelet factor 4 to fibrin would represent a large number of platelet factor 4 molecules per fiber.

CONCLUSIONS

It has been demonstrated that analysis of the kinetics of polymerization of fibrin by solution of the differential equations describing the reactions can be used to help interpret experimental results from electron microscopy or turbidity curves. These results reinforce the conclusion from earlier work that clot structure is, to a large extent, kinetically controlled. In other words, no external influences or additional mechanisms are necessary to account for most experimental observations; it is only necessary to postulate changes in the various rate constants.

In addition, more complex effects on assembly that are not intuitively obvious can be quantitatively modeled. For example, in experiments with platelet factor 4, increasing the rate of fiber aggregation is the only change that causes a slow rise in the final phase of the computed turbidity curves, with few other effects, as observed experimentally. In addition, such a mechanism could account for the very small amounts of platelet factor 4 that are effective. The effects of thrombospondin are unique in that it decreases both the lag period and the maximum turbidity simultaneously. Here again, the modeling is extremely helpful because the effects of increasing the rate of protofibril initiation are not intuitively obvious. Many other studies in the literature on fibrin assembly in a variety of conditions can be interpreted in terms of this scheme of assembly.

It is important to mention several cautionary notes related to both experimental data in this area and the modeling. The strengths and weaknesses or limitations of the experimental approaches must be recognized. Turbidity experiments must be very carefully done because the curves are especially sensitive to any small variations in conditions and subject to artifacts. In comparing curves, it is important that the amount of fibrin in the clot be identical in all experiments. There are two sorts of possible problems with observations by electron microscopy. Clots are relatively fragile structures that are subject to distortions during preparation for microscopy; an awareness of the numerous possible problems with different techniques is necessary. Also, by its nature electron microscopy involves sampling; it is important that many images from several preparations be examined to form any conclusions.

Furthermore, aspects of the model may be incorrect, and it is certainly incomplete. When you examine other kinetic modeling in the literature, it is apparent that this model is very complex with a great many adjustable parameters and the computations may seem almost intractable. On the other hand, with all that we know about fibrin polymerization, this model may seem to be hopelessly oversimplified. Many aspects have been omitted. For example, fibrinogen binding to fibrin, which is significant under certain conditions such as low thrombin concentrations, has not been included. Likewise, any cooperativity in the removal of fibrinopeptides is not included, and fibrinopeptide B cleavage has not been explicitly considered. There is also no explicit treatment of branching, although some conclusions may be drawn regarding branching, depending on the mechanism. The turbidity may not be strictly proportional to the size of the fibers under all conditions, because the number of fibers in the clot may also have an effect. However, this would only affect the beginning of the curves because the number of fibers reaches a plateau very quickly (Fig. 1 *h*).

Initially, we thought that it was better to err in the direction of oversimplification, to test the basic assumptions. Then, additional features can be added later. This success of this approach is borne out by the results: the limitations of each model are clear and the effects of changes are apparent. Also, the "simple" model accounts for a remarkable range of experimental observations. In addition, many of the rate constants are not known; it would be extremely useful to have experimental values for all of these parameters. However, this model can easily be modified to take any of these changes into account. On the other hand, kinetic studies do not provide direct information on mechanisms of assembly. For understanding mechanisms, biochemical and structural studies are necessary to define the binding sites involved and characterize other aspects of assembly.

The major strengths of kinetic modeling lie in identifying the consequences of a particular proposed mechanism or changes in some aspect of assembly on measured properties such as turbidity profiles or clot structure as observed by electron microscopy. Whenever more structural and biochemical data are available, suggesting further hypotheses regarding mechanisms of assembly, the consequences can be critically examined by modeling similar to that described here.

We thank Dr. M. Pring (Department of Physiology, University of Pennsylvania) for helpful discussions on the modeling of kinetic data, and are grateful to Drs. J. Holt and S. Niewiarowski (Thrombosis Research Center, Temple University School of Medicine) for gifts of platelet factor 4, and to Dr. G. Tuszynski (Department of Medicine, Medical College of Pennsylvania) for thrombospondin.

We acknowledge the support of National Institutes of Health grant HL30954.

Received for publication 29 May 1991 and in final form 12 March 1992.

REFERENCES

Bale, M. D., and D. F. Mosher. 1986. Effects of thrombospondin on fibrin polymerization and structure. *J. Biol. Chem.* 261:862–868.

Carr, M. E. 1986. Effect of hydroxylethyl starch on the structure of thrombin- and reptilase-derived fibrin gels. *J. Lab. Clin. Med.* 108:556–561.

Carr, M. E. 1988. Fibrin formed in plasma is composed of fibers more massive than those formed from purified fibrinogen. *Thromb. Haemostasis.* 59:535–539.

Carr, M. E., R. Cromartie, and D. A. Gabriel. 1989. Effect of homo poly(L-amino acids) on fibrin assembly: role of charge and molecular weight. *Biochemistry.* 28:1384–1388.

Carr, M. E., and D. A. Gabriel. 1980. Effect of dextran 70 on the structure of plasma-derived fibrin gels. *J. Lab. Clin. Med.* 96:985–993.

Carr, M. E., D. A. Gabriel, and J. McDonagh. 1986. Influence of Ca^{++} on the structure of reptilase-derived and thrombin-derived fibrin gels. *Biochem. J.* 239:513–516.

Carr, M. E., and J. Hermans. 1978. Size and density of fibrin fibers from turbidity. *Macromol.* 11:52–56.

Carr, M. E., M. Kaminski, J. McDonagh, and D. A. Gabriel. 1985. Influence of ionic strength, peptide release, and calcium ion on the structure of reptilase and thrombin-derived gels. *Thromb. Haemostasis.* 54:159–165.

Carr, M. E., G. C. White, and D. A. Gabriel. 1987. Platelet factor 4 enhances fibrin fiber polymerization. *Thromb. Res.* 45:539–543.

Dang, C. V., C. K. Shin, W. R. Bell, C. Nagaswami, and J. W. Weisel. 1989. Fibrinogen sialic acid residues are low affinity calcium-binding sites that influence fibrin assembly. *J. Biol. Chem.* 264:15104–15108.

Dhall, T. Z., W. A. Bryce, and D. P. Dhall. 1976. Effects of dextran on the molecular structure and tensile behavior of human fibrin. *Thromb. Haemostasis.* 35:737–745.

Erickson, H. P., and W. E. Fowler. 1983. Electron microscopy of fibrinogen, its plasmic fragments and small polymers. *Ann. NY Acad. Sci.* 408:146–163.

Ferry, J. D., and P. R. Morrison. 1947. Preparation and properties of serum and plasma proteins. VIII. The conversion of human fibrinogen to fibrin under various conditions. *J. Am. Chem. Soc.* 69:388–400.

Fowler, W. E., J. Hantgan, J. Hermans, and H. P. Erickson. 1981. Structure of the fibrin protofibril. *Biochemistry.* 78:4872–4876.

Gabriel, D. A., L. A. Smith, J. D. Folds, L. Davis, and S. E. Cancelosi. 1983. The influence of immunoglobulin (IgG) on the assembly of fibrin gels. *J. Lab. Clin. Med.* 101:545–552.

Galanakis, D. K., B. P. Lane, and S. R. Simon. 1987. Albumin modulates lateral assembly of fibrin polymers: evidence of enhanced fine fibril formation and of unique synergism with fibrinogen. *Biochemistry.* 26:2389–2400.

Hantgan, R., W. Fowler, H. Erickson, and J. Hermans. 1980. Fibrin assembly: a comparison of electron microscopic and light scattering results. *Thromb. Haemostasis.* 44:119–124.

Hantgan, R. R., and J. Hermans. 1979. Assembly of fibrin. A light scattering study. *J. Biol. Chem.* 254:11272–11281.

Hardy, J. J., N. A. Carrell, and J. McDonagh. 1983. Calcium ion function in fibrinogen conversion to fibrin. *Ann. NY Acad. Sci.* 408:279–287.

Holt, J. C. and S. Niewiarowski. 1989. Platelet basic protein, low affinity platelet factor 4 and β-thromboglobulin: purification and identification. *Methods Enzymol.* 169:224–233.

Janmey, P. A., L. Erdile, M. D. Bale, and J. D. Ferry. 1983. Kinetics of fibrin oligomer formation observed by electron microscopy. *Biochemistry.* 22:4336–4340.

Jones, M., and D. A. Gabriel. 1988. Influence of the subendothelial basement membrane components of fibrin assembly. *J. Biol. Chem.* 263:7043–7048.

Langer, B. G., J. W. Weisel, P. A. Dinauer, C. Nagaswami, and W. R. Bell. 1988. Deglycosylation of fibrinogen accelerates polymerization and increases lateral aggregation of fibrin fibers. *J. Biol. Chem.* 263:15056–15063.

Latallo, Z. S., A. P. Fletcher, N. Alkjaersig, and S. Sherry. 1962. Influence of pH, ionic strength, neutral ions, and thrombin on fibrin polymerization. *Am. J. Physiol.* 202:675–680.

Lewis, S. D., P. D. Shields, and J. A. Shafer. 1985. Characterization of the kinetic pathway for liberation of fibrinopeptides during the assembly of fibrin. *J. Biol. Chem.* 260:10192–10199.

Martinez, J., J. E. Palascak, and D. Kwasniak. 1977. Functional and metabolic properties of human asialofibrinogen. *J. Lab. Clin. Med.* 89:367–377.

Mosesson, M. W., J. P. DiOrio, M. F. Müller, J. R. Shainoff, J. R. Siebenlist, D. L. Amrani, G. A. Homandberg, J. Soria, S. Soria, and M. S. Samama. 1987. Studies on the ultrastructure of fibrin lacking fibrinopeptide B (β-fibrin). *Blood.* 69:1073–1081.

Medved', L., T. Ugarova, Y. Veklich, N. Lukinova, and J. Weisel. 1990. Electron microscope investigation of the early stages of fibrin assembly. Twisted protofibrils and fibers. *J. Mol. Biol.* 216:503–509.

Mihalyi, E. 1988. Clotting of bovine fibrinogen. Calcium binding to fibrin during clotting and its dependence on release of fibrinopeptide B. *Biochemistry.* 27:967–976.

Müller, M. Lasarcyk, and W. Burchard. 1981. Fibrinogen-fibrin transformation: 2. influence of temperature, pH and of various enzymes on the intermediate structures. *Int. J. Biol. Macromol.* 3:19–24.

Nair, C. H., and D. P. Dhall. 1991. Studies on fibrin network structure: the effect of some plasma proteins. *Thromb. Res.* 61:315–325.

Pirkle, H., P. Vukasin, I. Theodor, and D. Miyada. 1986. Relationship of final thickness of fibrin fibers to maximal rate of assembly and to fibrinopeptide B release. *In* Fibrinogen: fibrin Formation and Fibrinolysis. D. A. Lane, A. Henschen, M. K. Jasani, editors. Walter de Gruyter, Berlin. 69–75.

Sato, H., and A. Nakajima. 1984. Kinetic study of the initial stage of fibrinogen-fibrin conversion by thrombin (II) application of enzyme kinetics to turbidometrical method. *Thromb. Res.* 35:133–139.

Shah, G. A., C. H. Nair, and D. P. Dhall. 1987. Comparison of fibrin networks in plasma and fibrinogen solution. *Thromb. Res.* 45:257–264.

Shen, L. L., J. Hermans, J. McDonagh, and R. P. McDonagh. 1977. Role of fibrinopeptide release: comparison of fibrins produced by thrombin and ancrod. *Am. J. Physiol.* 232:H629–H633.

Smith, G. F. 1984. Fibrinogen: the specific thrombin substrate. *In* The Thrombin. Vol. 1. R. Machovich, editor. CRC Press, Boca Raton, FL. 55–82.

Tuszynski, G. P., V. L. Rothman, A. Murphy, and K. A. Knudsen. 1987. Role of thrombospondin in hemostasis and cell adhesion. *Semin. Thromb. Hemostasis.* 13:361–368.

Voter, W. A., C. Lucaveche, and H. P. Erickson. 1986. Concentration of protein in fibrin fibers and fibrinogen polymers. *Biopolymers.* 25:2375–2384.

Weisel, J. W. 1986*a*. The electron microscope band pattern of human fibrin: various stains, lateral order, and carbohydrate localization. *J. Ultrastruct. Mol. Struct. Res.* 96:176–188.

Weisel, J. W. 1986*b*. Structural studies of fibrin assembly: lateral aggregation and the role of the two pairs of fibrinopeptides. *Biophys. J.* 50:1079–1093.

Weisel, J. W. 1988. Structural studies of lateral aggregation in fibrin assembly. *In* Fibrinogen 3. Biochemistry, Biological Functions, Gene Regulation and Expression. M. W. Mosesson, D. L. Amrani, K. R. Siebenlist, and J. P. DiOrio, editors. Elsevier Science Publishers, New York. 113–116.

Weisel, J. W., C. V. Stauffacher, E. Bullitt, and C. Cohen. 1985. A

model for fibrinogen: domains and sequence. *Science (Wash. DC)*. 230:1388–1391.

Wilf, J., J. A. Gladner, and A. P. Minton. 1985. Acceleration of fibrin gel formation by unrelated proteins. *Thromb. Res.* 37:681–688.

Wilf, J., and A. P. Minton. 1986. Soluble fibrin-fibrinogen complexes as intermediates in fibrin gel formation. *Biochemistry.* 25:3124–3133.

Wolfe, J. K., and D. F. Waugh. 1981. Relations between enzymatic and association reactions in the development of bovine fibrin clot structure. *Arch. Biochem. Biophys.* 211:125–142.